RSC Advances

Metabolic variation of HeLa cells migrating on microfabricated cytophilic channels studied by fluorescence lifetime of NADH

Journal:	*RSC Advances*
Manuscript ID:	RA-COM-07-2014-006492.R2
Article Type:	Communication
Date Submitted by the Author:	04-Sep-2014

Complete List of Authors:	Deka, Gitanjal; National Yang Ming University, Institute of Biophotonics Okano, Kazunori; National Chiao Tung University, Laser Bio/Nano Laboratories Department of Applied Chemistry and Institute of Molecular Science Masuhara, Hiroshi; National Chiao Tung University, Hsinchu, Taiwan, Depertment of Applied Chemistry and Institute of Molecular Science Li, Yaw-Kuen; National Chiao Tung University, Hsinchu, Taiwan, Depertment of Applied Chemistry and Institute of Molecular Science Kao, Fu-Jen; National Yang Ming University, Institute of Biophotonics

This manuscript reports an *in situ* surface-modification of a substrate by laser ablation for monitoring metabolic physiology of migrating cells through guided channels.

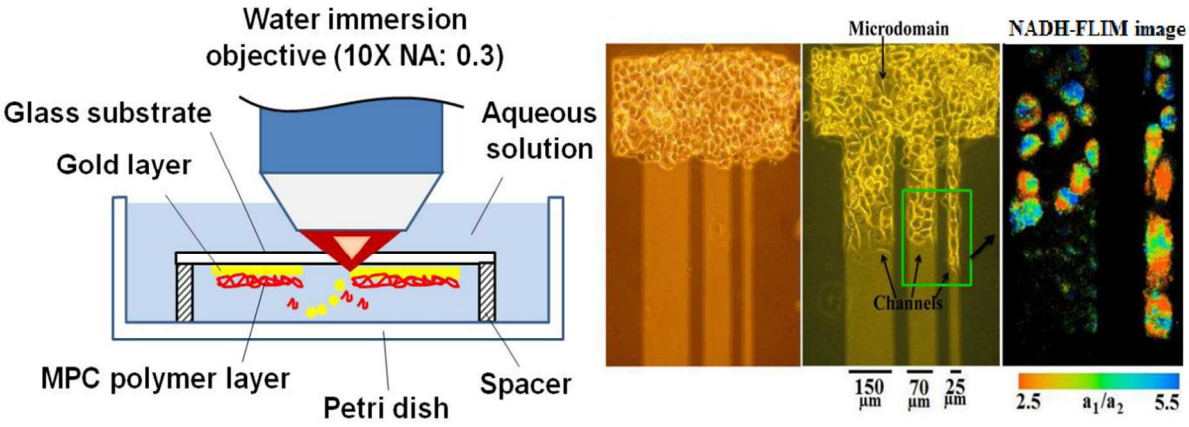

RSC Advances RSCPublishing

COMMUNICATION

Metabolic variation of HeLa cells migrating on microfabricated cytophilic channels studied by fluorescence lifetime of NADH

Cite this: DOI: 10.1039/x0xx00000x

Received ooth ,

Accepted ooth

DOI: 10.1039/x0xx00000x

www.rsc.org/

Gitanjal Deka,[a†] Kazunori Okano,[b†*] Hiroshi Masuhara,[c] Yaw-Kuen Li[c] and Fu-Jen Kao[a*]

We report a novel method for studying cellular migration *in vitro*. Cytophilic microdomains were formed on a cytophobic substrate by laser ablation. HeLa cells were grown on those domains until confluence, and then channels were formed to guide cellular migration. Two-photon excitation fluorescence-lifetime imaging of NADH revealed the metabolic variation among migrating and nonmigrating cells.

The movement and collective migration of cells are crucial to physiological and biological processes such as development, wound healing, and cancer invasion.[1] Cells can exhibit various modes of collective migration for various physiological purposes. For example, epithelial cells migrate during wound healing, and tumor cells invade surrounding tissues.[1,2] Previous studies *in vivo* and *in vitro* have suggested that geometrical boundaries influence the way of migration of those cells.[3] Furthermore, migration in various geometries gives rise to diverse morphological behaviors.[3] Although the mechanical and physical behaviors of migrating cells have been extensively studied with reference to actomyosin organization, orientation and traction forces, the internal energetic processes of migrating cells remains mostly unexplored. More specifically, the metabolic activity of cancer cells during invasion and intravasation is crucial to the control and diagnosis of cancer formation and growth[4].

Micro culture devices have been used widely for studying cell patterning, cell trapping and even specific cell migration.[5] To satisfy certain requirements of cellular migration, the prepared cell adhesive patterns may have to be dynamically altered to yield cell-cell interactions while cells are growing. The dynamic control of cell adhesive activity on solid surfaces by heat, electric potential, enzymatic reactions, and irradiation of light has attracted

considerable interest.[5] The position-specific removal of surface materials by laser ablation to form arrays of bio-molecules and cells is an emerging approach in quantitative biomedicine.[6] Our group previously demonstrated quick cellular patterning by laser ablation using Q-switched neodymium-doped yttrium orthovanadate ($Nd:YVO_4$) laser.[7] The use of a laser is favourable. When set at an average power of 5 mW, it modifies an area of diameter approximately 8~10 μm around the focal spot. In this work, the same approach was applied to form micro colonies of HeLa cells (uterocervical cancer cells) and to investigate their migration.

The metabolic physiology of cancer cells crucially affects their growth and invasion into surrounding tissues. Reduced nicotinamide adenine dinucleotide (NADH) is a metabolic coenzyme for both glycolysis and oxidative phosphorylation and a principal electron donor in adenosine triphosphate (ATP) production.[8] The NADH molecule has two functional forms, free and protein bound, with different fluorescence lifetimes of ~0.4 ns and 2.5 ns, respectively.[8,9] Fluorescence lifetime imaging (FLIM) can be used to determine the relative concentration of the functional states (a_1 and a_2 for free and protein-bound NADH, respectively. These values depend on cellular environmental conditions, such as temperature, viscosity, pH and independent of excitation wavelength and laser power. For measurement procedures see data analysis section in Supplementary Information.) of this coenzyme, and their lifetimes, by fitting the fluorescence decay to a double exponential model.[10] Bound NADH transfers electrons to O_2 molecules in the ATP production. Accordingly, the binding of NADH to protein is associated with the generation of energy, and the relative quantities of free and bound species provide information on the relative energy metabolic state of cells. One of the hallmarks of carcinogenesis is a shift of the cellular metabolic pathway from oxidative phosphorylation to glycolysis in the production of ATP (Warburg effect).[11] NADH-FLIM is a promising method for diagnosing this dynamical shift to glycolysis, which causes a relative increase in the amount of free NADH.[11] Reports have suggested that non-metastatic cells exhibit large shifts in metabolic pathways while the pathways of metastatic cells differ only slightly from those of normal cells.[10]

In this study, the migrating invasive and the static noninvasive conditions of cancerous cells were mimicked by allowing HeLa cells at confluence state to migrate along micro-fabricated channels of different widths. Cells under crowded condition in a fabricated micro-sized domain were under oxidative and mechanical stress, whereas migrating cells had more available space. The effect of cell density on energy metabolism has been investigated earlier.[12] Our group previously evaluated the metabolism of HeLa cells *in vitro* in various stages of cell growth including early, mid-logarithmic, and confluent.[10] Skala *et al.* also performed an *in vivo* study of the metabolism of cancerous and precancerous epithelia.[13] Those studies suggested that the relative concentration of bound NADH in confluent cells and cancerous tissues is lower than that in growing cells and normal tissues.[13,14] This effect has been explained as being caused by a decrease in the concentration of available oxygen in the cells, limiting the oxidative phosphorylation and shifting the energy metabolism to glycolysis.[12] This work reports an NADH-FLIM-based mapping of the metabolic physiology of migrating cells in relation to that of non-migrating cells. A Ti:sapphire femtosecond pulsed laser (200 fs, 76 MHz) was utilized to achieve NADH two-photon fluorescence emission. FLIM data were obtained by time-correlated single photon counting (TCSPC) technique.

$Nd:YVO_4$ laser-directed (lasing at 1064 nm) microfabrication technique was used to fabricate microdomains for cell colonies over a cytophobic-surfaced glass substrate. Those cell colonies were used to investigate the intercellular metabolic physiology of collective cell migration along microfabricated channels *in vitro*. The substrate was

fabricated by coating a thin gold layer on a glass slide and over-layering with cytophobic 2-methacryloxyethylphosphorylcholine (MPC) polymer (NOF Corporation, Tokyo, Japan). MPC polymer coated surface contains stable intramolecular zwitterions that interact minimally with materials that have both negative and positive charges like proteins and living cells. Meanwhile, the protein adsorption is deeply affected by water molecules on the substrate.[15] The MPC polymer layer is highly hydrated with free water molecules that interact weakly with the MPC polymer, resulting its proteinphobic and cytophobic characteristics.[15] The gold layer served as the thermal transducer to achieve photothermal ablation. At the focal point of the laser, the transducer layer absorbed light and produced much heat locally. This heat depleted the transducer layer along with the cytophobic polymer exposing the cytophilic glass surface. The laser microfabrication system comprised of an Nd:YVO_4 laser, a piloting diode laser (653 nm), a pair of scanning galvano meter mirrors and a 10× water immersion objective lens with a numerical aperture of 0.3 [Supplementary Fig. 1]. Thus, the diameter of the beam spot, defined by the boundary of the I_0/e^2 Gaussian beam, was 3.4 μm. The laser beam was vector-scanned for pattern drawing using the galvano mirrors. The beam scanning speed was 300 μm/s under the objective, which allowed the patterning of a domain approximately the size of 150×1000 μm^2 within 60 seconds [Supplementary Video 1]. Finally, HeLa cells were seeded to form cell colonies on the microfabricated domains, and the fabricated channels that connected to the domain would induce the migration. The observations were carried out using a two-photon laser-scanning microscope. The Ti:sapphire laser excited cellular NADH through two-photon absorption in the wavelength range of 730~740 nm [Supplementary Fig.2]. The emitted fluorescence was collected by an appropriate dichroic mirror that reflected wavelengths in the range 450-475 nm. SPCM and SPCImage software's (Becker and Hickel, GmbH, Germany) were used to acquire and analyze the data, respectively.

Microdomains were fabricated by the photothermal ablation of the gold and the MPC polymer films by spot heating using a focused laser beam, exposing the cell-adhesive surface. However, the molten gold quickly solidified and scattered around the fabricated area, leaving gold particles (sized from tens to several hundred nanometers) as debris. The gold particles exhibit broad-band emission spectra. Due to surface plasmon resonance, they may also enhance the fluorescence emission of some molecules that are present in the cell culture medium, which could interfere with the measurement of the NADH fluorescence. To reduce the gold debris on the surface, the laser ablation was carried out with the gold and polymer layer side facing down and the glass surface facing the incoming laser beam [Fig. 1 (a) and Supplementary video 2]. Figure 1 (b) Transmission illumination, (c) scanning electron (SEM), and (d) atomic force (AFM) microscopy images present details of the ablated area. The transmission illumination depicted clear laser ablated domains distinct from surrounding. In the SEM image, the bright region indicates the metallic gold that has the high density of electrons. In contrast, the dark region lacks electrons, indicating the removal of the gold layer. AFM showed the center of laser treated domain was flat, although tall peaks were detected at the edges of the domain resulting from laser ablation. During laser microfabrication, the aqueous medium at room temperature helped to solidify the gold debris rapidly. With the gold and polymer layers coated side facing down, the gold particles would drop from the glass substrate toward the bottom of the petri-dish due to gravity, preventing them from adhering to the substrate [Supplementary video 2]. In contrast the gold debris remained on the surface, if the substrate was held with the gold and polymer layer upward facing the laser [Supplementary Fig. 3]. This improvement in laser ablation

enables the successful autofluorescence imaging of cellular NADH. Highly contrasted images of cells were obtained owing to the absence of gold debris [Fig. 1e]. For comparison, the gold debris interfered cell image was shown in Fig. 1f.

A cell-adhesive rectangular domain (150 μm × 1 mm) was formed on the cytophobic substrate. HeLa cells were seeded, and a cellular mono layer was cultured for two days. After the domain was filled with cells, strip channels with three widths of 150 μm, 70 μm and 25 μm, and each had a length of 550 μm were formed *in situ* [Fig. 2 a, b]. Cells were observed to migrate along channels under FLIM. Cells migrate faster in 25 μm channel. Migration speed and morphologies of cells were same in both 150 and 70 μm. Along with migration, there may also be contribution from cell culture spreading. However, cells moved to the channels despite of there was enough free space in the source domain to grow. Additionally, vacant space appeared in the source domain during the cell movement [Supplementary Fig. 4], which indicates that the cell migration played a major role in these series of experiments. The metabolic physiology of cells that migrated along these two channels was studied simultaneously after 32 h of channel formation. Figures 2c and 2d are representative images of NADH autofluorescence and the NADH free to protein-bound (a_1/a_2) ratio [a_1: free NADH contribution, a_2: bound NADH contribution (in equation 1 of supplementary information)] FLIM images, respectively. The measurements of a_1/a_2 were made by taking the region of interest from the cytosol only, omitting the nuclear regions (which appeared blue in the FLIM images owing to presence of a trace amount of free NADH) and extra cellular regions. Higher contribution of bound NADH was observed in the migrating cells along the channels than in the cells resting inside the rectangular domain [Table 1]. Cells at the leading edge exhibited the highest contribution of bound form with an a_1/a_2 ratio of 2.4~2.8, which is similar to that of cells in the normal culture dish. Following cells of the front cells, which had being migrating, had an a_1/a_2 ratio of ≈3.2. A comparison of the a_1/a_2 ratio among migrating cells along two different channels revealed that the front cells in the narrower channel had a higher bound form NADH contribution (a_1/a_2 ≈2.4) than those on the wider channel (a_1/a_2 ≈2.8~3.1). The cells at rest inside the rectangular domain had the lowest bound form contribution (a_1/a_2 ≈3.8). Notably, the a_1/a_2 ratio is inversely related to the metabolic activity or represents shift in metabolic pathways from oxidative phosphorylation to glycolysis in direct relation for cancer growth.[10, 13]

When the cells grow to confluence, the cell density is high and the average surface area for each cell attached to the substrate is relatively small. This condition generates a mechanical and oxidative stress on the cells, which reduces metabolic activity (decreased contribution of bound NADH). Thus it is still unclear whether the a_1/a_2 variation depends on migration or the stress, or both of them. Figure 3 presents the cells under non-migration condition in closed microdomains, with the same width to the channels, where the cells also grew to confluence. According to the results herein, cells in a narrower microdomain (with a width that was comparable to the size of a cell) had a greater stress and therefore exhibited lower bound form NADH contribution [Fig. 3, Table 1] Cells remaining in closed microdomains of width 25 and 70 μm had a_1/a_2 ration ranging 3.9~4.0 that was comparable to the cells in densely populated wider rectangular domains having channels [Table 1]. Summarizing the results, in the narrow channel, only one cell was located at the leading edge and had a higher contribution of bound NADH than that of the front cells in wider channel. Cells in a narrower channel migrated faster [Fig. 2b], requiring higher energy and thus enhanced metabolism. In wider channel, the leading edge contained more than one cell to pull the entire cohort of cells. However, the follower cells in both channels

exhibited similar ratios of free to bound NADH contribution. The comparable values of cellular a_1/a_2 in a normal glass bottom dish to that of the front cells are attributed to the freedom of migration of the latter. The cells may move toward areas of lower density in search of stronger attachment and higher stability that improves their metabolic activity. Furthermore consequent drop in oxidative stress may have shifted the metabolic pathway from glycolysis to oxidative phosphorylation, increasing the proportion of the bound form of NADH inside the cell. The change in hypoxic condition may be partially responsible for the observed change in the relative concentrations of the protein-bound and free NADH species. The relative concentrations of those species also depend on the speed of migration, cell morphology and cytoskeleton.

Conclusions

This work proposes a microfabrication method based on laser ablation for studying the migration of cancer cells. The relative metabolic physiologies of cells that migrate along channels with different widths and of non-migrating cells are mapped and compared with each other. Migrating cells exhibit a higher bound form NADH contribution than the non-migrating ones, with the front cells exhibit the highest contribution. This study provides information on the metabolic energetic conditions of migrating cancer cells. The presented laser ablation-based *in-situ* surface-modification coupled with autofluorescence analysis of the cells has valuable applications in the studies of cell migration and chemotaxis, which include the effect of ECMs and other proteins and chemicals. For instance, dermal cells are a key that facilitates wound closure and the contraction of the wound edge during healing. The cells from wound sites can be collected and grown on the substrate to observe the migratory mechanism. The microfabrication technique is also applicable to test effects of external drugs on the migration, while FLIM may help to elucidate such drug effects in response to migration control. Migration of cancerous cells on fabricated channels has the potential to serve as a model of cancerous cells invasion on normal tissues[16]. The physical space seems critical to such cellular migration in general. There is a report that young neurons change position by migrating through astrocyte tunnels[17]. Similar to these phenomena *in vivo*, control of cell migration on a patterned substrate and monitoring NADH shown in the present manuscript shall be useful for the study of cell reorganization in tissues.

Acknowledgements

We acknowledge the help from MOST, Taiwan for financially supporting the work under the grant [FJK (MOST-102-2112-M-010-003-MY3), KO (MOST-103-2320-B-009-001MY2)]. Dr. How Foo Chen is acknowledged for his help in obtaining the gold slide. Grammatical and writing style errors in the original version have been corrected by our colleague Mr. Ted Knoy, who is a native English speaker.

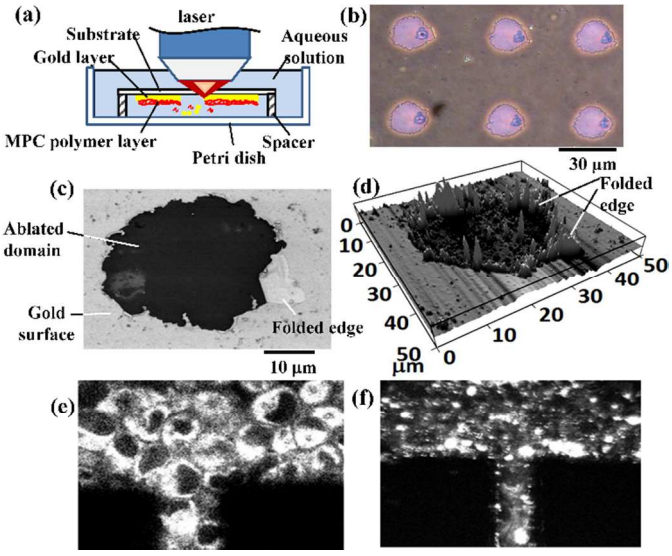

Fig. 1 Laser-ablated microdomain. (a) Schematics of laser ablation in aqueous solution. (b) Wide field, (c) SEM, and (d) AFM images of ablated domains, respectively. (e) and (f) Autofluorescence images of HeLa cells in ablated domains. The substrates (b–e) were

ablated by the method depicted in (a). In the case of image (f), the substrate was positioned with the gold and MPC polymer layer held upward facing the laser. (See Supplementary Fig. 3 "gold and MPC polymer layer held upward facing the laser from top").

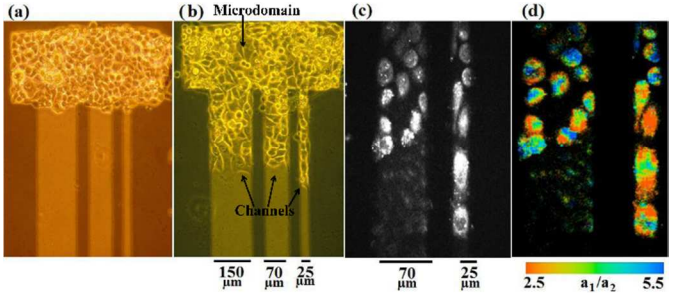

Fig. 2 Representative images of cell migration in channels. (a) Wide field micrograph of confluent HeLa cells in ablated rectangular domain. Channels had already formed. (b) Wide field micrograph of cells at 32 h incubation after forming the channels. (c) NADH autofluorescence image of migrating cells at 32 h incubation after forming the channels. (d) FLIM image showing a_1/a_2 at 32 h incubation after forming the channels. The a_1/a_2 represents the relative value of NADH free to protein bound form, respectively, which are calculated by a method indicated in Supplemental information.

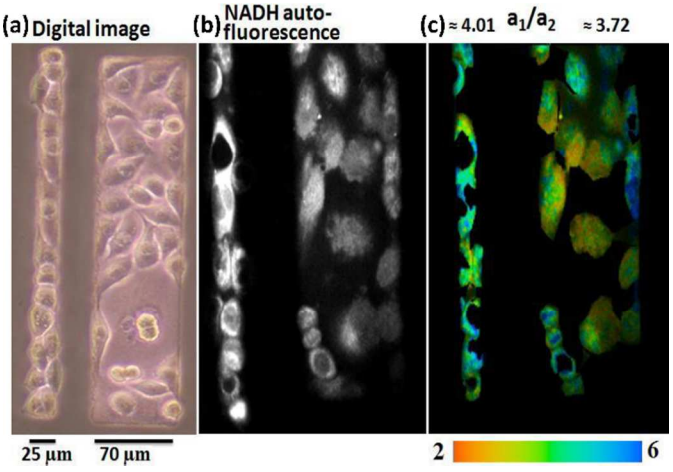

Fig. 3 Representative images of resting cells in closed microdomains of two different geometries having similar width to the cell migrating channels. (a) Wide field micrograph of HeLa cells in closed microdomains; (b) NADH autofluorescence image of HeLa cells in same sized microdomain; (c) FLIM image showing a_1/a_2 obtained from FLIM signals of same HeLa cells.

Closed microdomain		Rectangular domain with channels						Dish
25 μm	70 μm	25 μm			70 μm			
		Front*	Follower*	Domain*	Front*	Follower*	Domain*	
4.0 ±0.15	3.9 ±0.12	2.4 ±0.1	3.4 ±0.12	3.8 ±0.18	2.8 ±0.08	3.4 ±0.17	3.8 ±0.2	2.5 ±0.3

Table 1: NADH free to protein-bound ratio (a_1/a_2) given by FLIM analysis of HeLa cells on closed microdomains having 25 and 70 μm wide (left), rectangular domain (150 μm × 1 mm) with channels of 25 and 70 μm wide (middle), and conventional glass bottom dish of 35 mm (right). *Front, *follower, and *domain mean migrating front cells, cells following front cells, and cells remained in rectangle domain.

Notes and references

[a] *Institute of Biophotonics, National Yang-Ming University, Linong St. Sec 2, No. 155, Taipei, Taiwan. Ph: +886-02-28267000 (5713)*

[b] *Centre for Interdisciplinary Science; National Chiao Tung University, Tin-Ka Ping Photonics Centre, 1001 Ta Hsueh Rd., Hsinchu 30010, Taiwan.*

[c] *Department of Applied Chemistry and Institute of Molecular Science, National Chiao Tung University, Tin-Ka Ping Photonics Centre, 1001 Ta Hsueh Rd., Hsinchu 30010, Taiwan.*

*Corresponding email address: fjkao@ym.edu.tw, okano@nctu.edu.tw

†These authors contributed equally to this work.

1. P. Friedl, and D. Gilmour, *Nat. Rev. Mol. Cell. Biol.*, 2009, 10, 445—457.

2. O. Ilina, and P. Friedl, *J. Cell. Sci.* 2009, 122, 3203—3208.
3. S. R. K. Vedula, M. C. Leong, T. L. Lai, P. Hersen, A. J. Kabla, C. T. Lim, and B. Ladoux, *Proc. Natl. Acad. Sci. USA,* 2012, 109, 12974—12979; M. Poujade, E. Grasland-Mongrain, A. Hertzog, J. Jouanneau, P. Chavrier, B. Ladoux, A. Buguin, and P. Silberzan, *Proc. Natl. Acad. Sci. USA,* 2007,104, 15988—15993.
4. J. M. Jessup, P. Battle, H. Waller, K. H. Edmiston, D. B. Stolz, S. C. Watkins, J. Locker, and K. Skena, *Cancer Res.* 1999, 59, 1825-1829; C. Li and R. M. Jackson, *Am. J. Physiol. -Cell Physiol.* 2002, 282, C227-C241.
5. J. Nakanishi, K. Yamaguchi, and M. Maeda, *Anal. Sci.* 2008, 24, 67—72.
6. K. Okano, D. Yu, Y. Maezawa, Y. Hosokawa, A. Kira, M. Matsubara, I. Liau, and H. Tsubokawa, H. Masuhara, *ChemBioChem,* 2011, 12, 795—801; K. Okano, A. Matsui, Y. Maezawa, P.-Y. Hee, M. Matsubara, H. Yamamoto, Y. Hosokawa, H. Tsubokawa, Y.-K. Li, F.-J. Kao and H. Masuhara, *Lab. Chip,* 2013, 13, 4078—4086; T. Kaji, S. Ito, H. Miyasaka, Y. Hosokawa, H. Masuhara, C. Shukunami, and Y. Hiraki, *Appl. Phys. Lett.,* 2007, 91, 023904.
7. G. Deka, K. Okano, and F. J. Kao, *J. Biomed. Opt.,* 2014, 19, 011012.
8. J. R. Lakowicz, *Principles of fluorescence spectroscopy*, Springer (2009).
9. A. Gafni and L. Brand, *Biochemistry,* 1976, 15, 3165—317; W. Becker, A. Bergmann, M. A. Hink, K. König, K. Benndorf, C. Biskup, *Microsc. Res. Technol.* 2004, *63*, 58—66.
10. V. V. Ghukasyan and F.-J. Kao, *J. Phys. Chem. C*, 2009, 113, 11532—11540; A. Pradhan, P. Pal, G. Durocher, L. Villeneuve, A. Balassy, F. Babai, L. Gaboury, and L. Blanchard, *J. Photochem. Photobiol. B,* 1995, 31, 101—12; W. Becker, A. Bergmann, M. A. Hink, K. König, K. Benndorf, C. Biskup, *Microsc. Res. Technol.,* 2004, 63, 58—66.
11. O. Warburg, F. Wind, and E. Negelein, *J. Gen. Physiol.,* 1927, 8, 519—530.
12. J. Bereiter-Hahn, A. Munnich, and P. Woiteneck, *Cell. Structure. Funct.*, 1998, 23, 85—93.
13. M. C. Skala, K. M. Riching, D. K. Bird, A. Gendron-Fitzpatrick, J. Eickhoff, K. W. Eliceiri, P. J. Keely, and N. Ramanujam, *J. Biomed. Opt*., 2007, 12, 024014.
14. K. D. Bird, L. Yan, M. K. Vrotsos, K. W. Eliceiri, E. M. Vaughan, P. J. Keely, J. G. White, and N. Ramanujam, *Cancer Res.,* 2005, 65, 8766-8773; M. C. Skala, K. M. Riching, A. Gendron-Fitzpatrick, J. Eickhoff, K. W. Eliceiri, J. G. White, and N. Ramanujam, *Proc. Natl. Acad. Sci. USA,* 2007, 104, 19494-19499.
15. K. Ishihara, H. Nomura, T. Mihara, K. Kurita, and Y. Iwasaki, *J. Biomed. Mater. Res. Part A*, 1998, 39, 323—330; Y. Xu, M. Takai, and K. Ishihara, *Biomaterials*, 2009, 30, 4930—4938.
16. K. Yuan R. K. Singh, Gabriel Rezonzew, and Gene P. Siegal, "*In vitro* matrices for studying tumor cell invasion" chapter 2 in *cell motility in cancer invasion and metastasis*, Springer, Dordrecht, The Nederland's, 2006.
17. N. Kaneko, O. Marin, M. Koike, Y. Hirota, Y. Uchiyama, J. Y. Wu, Q. Lu, M. Tessier-Lavigne, A. Alvarez-Buylla, H. Okano, J. L. R. Rubenstein, and K. Sawamoto, *Neuron* 67, 2010, 213–223.